

# Elliptic flow and nearly perfect fluidity in dilute Fermi gases

Thomas Schäfer

*Department of Physics, North Carolina State University, Raleigh, NC 27695*

**Abstract.** In this contribution we summarize recent progress in understanding the shear viscosity of strongly correlated dilute Fermi gases. We discuss predictions from kinetic theory, and show how these predictions can be tested using recent experimental data on elliptic flow. We find agreement between theory and experiments in the high temperature regime  $T \gg T_F$ , where  $T_F$  is the temperature where quantum degeneracy effects become important. In the low temperature regime,  $T \sim T_F$ , the strongest constraints on the shear viscosity come from experimental studies of the damping of collective modes. These experiments indicate that  $\eta/s \lesssim 0.5\hbar/k_B$ , where  $\eta$  is the shear viscosity and  $s$  is the entropy density.

**Keywords:** quantum fluids, hydrodynamics, strong correlations.

**PACS:** 03.75.Ss, 05.60.Gg, 67.90.+z.

## INTRODUCTION

Experiments carried out at the relativistic heavy ion collider (RHIC) have demonstrated that the quark gluon plasma is a very good fluid [1, 2, 3]. A quantitative analysis of the observed elliptic flow in the framework of viscous relativistic hydrodynamics shows that [4, 5]

$$\frac{\eta}{s} \lesssim 0.5 \frac{\hbar}{k_B} \quad (1)$$

where  $\eta$  is the shear viscosity and  $s$  is the entropy density. The best fit to the data corresponds to even smaller values,  $\eta/s \simeq (0.1 - 0.2)\hbar/k_B$ . This number is close to a proposed lower bound,  $\eta/s = \hbar/(4\pi k_B)$ , on the ratio of shear viscosity to entropy density that is saturated in the strong coupling limit of a large class of field theories that can be analyzed using the AdS/CFT correspondence [6, 7].

The RHIC results raise the question whether nearly perfect fluidity is a phenomenon that is specific to relativistic gauge theories, or whether it is a more general effect that also appears in other strongly correlated quantum fluids. If that is the case we may also ask whether there are universal aspects of nearly perfect fluidity that go beyond the relation  $\eta/s \simeq \hbar/(4\pi k_B)$ . Other universal features could include bounds on other transport coefficients like diffusion constants or relaxation times, or constraints on spectral properties of the theory. In the context of interpreting the RHIC results we are particularly interested in the question whether nearly perfect fluidity is consistent with a quasi-particle description of the fluid.

Cold, dilute Fermi gases in which the interaction between the atoms can be tuned using an external magnetic field provide a new paradigm for strongly correlated quantum fluids [8, 9, 10]. These systems have been realized experimentally using optically trapped alkali atoms such as  ${}^6\text{Li}$  and  ${}^{40}\text{K}$ . These two atoms are fermions be-

cause they possess a single valence electron and the nuclear spin is integer. When a dilute gas of alkali atoms is cooled to very low temperature, we can view the atoms as pointlike particles interacting via interatomic potentials which depend on the hyperfine quantum numbers of the valence electron. A Feshbach resonance arises if a molecular bound state in a “closed” hyperfine channel crosses the threshold of an energetically lower “open” channel. Because the magnetic moments of the states in the open and closed channel are in general different, Feshbach resonances can be tuned using an applied magnetic field. At resonance the two-body scattering length in the open channel diverges, and the cross section  $\sigma$  is limited only by unitarity,  $\sigma(k) = 4\pi/k^2$  where  $k$  is the relative momentum.

In the unitarity limit details of the microscopic interaction are irrelevant, and the system displays universal properties. The dilute Fermi gas can be described by the effective lagrangian

$$\mathcal{L} = \psi^\dagger \left( i\partial_0 + \frac{\nabla^2}{2m} \right) \psi - \frac{C_0}{2} (\psi^\dagger \psi)^2, \quad (2)$$

where  $\psi$  is a two-component fermion field with mass  $m$ . The coupling constant  $C_0$  is related to the  $s$ -wave scattering length  $a$ . The precise form of this relation depends on the regularization scheme. In dimensional regularization one finds  $C_0 = (4\pi a)/m$ . Terms with more derivatives or higher powers of the field are related to effective range corrections, higher partial waves, and many-body forces. All of these terms are irrelevant in the universal limit. The two-body scattering cross section is

$$\sigma(k) = \frac{4\pi a^2}{1 + a^2 k^2}. \quad (3)$$

In the limit  $a \rightarrow \infty$  the theory is parameter free, strongly interacting and scale as well as conformally invariant.

## THERMODYNAMICS

In the weak coupling limit  $a \rightarrow 0$  the equation of state of the dilute Fermi gas is that of a free two-component Fermi gas,

$$P_0(\mu, T) = -2T\lambda_{dB}^{-3} Li_{5/2}(-\zeta^{-1}), \quad (4)$$

where  $\lambda_{dB} = [(2\pi)/(mT)]^{1/2}$  is the de Broglie wave length,  $Li_\alpha(x)$  is the Polylogarithm function, and  $\zeta = \exp(-\mu/T)$  is the fugacity. At unitarity scale invariance implies that the equation of state is of the form

$$P(\mu, T) = \frac{h(\zeta)}{2} P_0(\mu, T), \quad (5)$$

where  $h(\zeta)$  is a universal function. This function can be calculated using the Virial expansion at high temperature,  $\zeta \gg 1$ , but it is a non-perturbative quantity at low temperature. The equation of state is known to about 10% from experimental measurements [11, 12, 13] and quantum Monte Carlo simulations [14, 15, 16]. At zero temperature  $h(0)/2 = \xi^{-3/2}$ , where  $\xi \simeq 0.4$  is known as the Bertsch parameter. Scale invariance also implies that

$$P = \frac{2}{3} \varepsilon, \quad (6)$$

where  $\varepsilon$  is the energy density. At low temperature the attractive interaction between the fermions leads to superfluidity. The critical temperature is  $T_c \simeq 0.15E_F$  [15], where  $E_F$  is the Fermi energy. The Fermi energy of the interacting gas is defined by  $E_F = k_F^2/(2m)$  where  $k_F = (3\pi^2 n)^{1/3}$  is the Fermi momentum and  $n$  the fermion density.

## HYDRODYNAMICS

At large distances and long times deviations from equilibrium are described by hydrodynamics. For simplicity we will consider the unitary Fermi gas in the normal phase. In that case there are five hydrodynamic variables, the mass density  $\rho = mn$ , the flow velocity  $\vec{v}$ , and the energy density  $\mathcal{E}$ . These variables satisfy five hydrodynamic equations, the continuity equation, the Navier-Stokes equation, and the equation of energy conservation,

$$\frac{\partial \rho}{\partial t} + \vec{\nabla} \cdot (\rho \vec{v}) = 0, \quad (7)$$

$$\frac{\partial (\rho v_i)}{\partial t} + \nabla_j \Pi_{ij} = 0, \quad (8)$$

$$\frac{\partial \mathcal{E}}{\partial t} + \nabla_i j_i^\mathcal{E} = 0. \quad (9)$$

The total energy density is the sum of the internal energy density and kinetic energy density,  $\mathcal{E} = \varepsilon + \frac{1}{2} \rho v^2$ . These

equations close once we supply constitutive relations for the stress tensor  $\Pi_{ij}$  and the energy current  $j_i^\mathcal{E}$  as well as an equation of state. As explained in the previous section the equation of state is  $P = \frac{2}{3} \varepsilon$ . The stress tensor is given by

$$\Pi_{ij} = \rho v_i v_j + P \delta_{ij} + \delta \Pi_{ij}, \quad (10)$$

where  $\delta \Pi_{ij}$  is the dissipative part. The dissipative contribution to the stress tensor is  $\delta \Pi_{ij} = -\eta \sigma_{ij}$  with

$$\sigma_{ij} = \left( \nabla_i v_j + \nabla_j v_i - \frac{2}{3} \delta_{ij} (\nabla_k v_k) \right), \quad (11)$$

where  $\eta$  is the shear viscosity and we have used the fact that the bulk viscosity of the unitary Fermi gas is zero [17]. The energy current is

$$j_i^\mathcal{E} = v_i w + \delta j_i^\mathcal{E}, \quad (12)$$

where  $w = \varepsilon + P$  is the enthalpy density. The dissipative energy current is

$$\delta j_i^\mathcal{E} = \delta \Pi_{ij} v_j - \kappa \nabla_i T, \quad (13)$$

where  $T$  is the temperature and  $\kappa$  is the thermal conductivity. We note that the temperature  $T = T(n, P)$  is a function of the density  $n = \rho/m$  and the pressure. In order to determine  $T$  we need the equation of state in the form  $P = P(n, T)$ . Universality implies that  $P(n, T) = m^{-1} n^{5/3} f(mT/n^{2/3})$  where  $f(x)$  is a universal function that is related to the function  $h(\zeta)$  defined in equ. (5). The situation simplifies in the high temperature limit where  $P = nT$ . Universality also restricts the dependence of the shear viscosity and thermal conductivity on the density and the temperature. We can write

$$\eta(n, T) = \alpha_n \left( \frac{mT}{n^{2/3}} \right) n, \quad (14)$$

$$\kappa(n, T) = \sigma_n \left( \frac{mT}{n^{2/3}} \right) \frac{n}{m}, \quad (15)$$

where  $\alpha_n(y)$  and  $\sigma_n(y)$  are universal functions of  $y = mT/n^{2/3}$ . The relative importance of thermal and momentum diffusion can be characterized in terms of a dimensionless ratio known as the Prandtl number,  $Pr = c_p \eta / (\rho \kappa)$ , where  $c_p$  is the specific heat at constant pressure. In the high temperature limit  $c_p = \rho/m$  and  $Pr = \alpha_n / \sigma_n$ . Kinetic theory predicts that in this limit  $Pr = 2/3$  [18].

## KINETIC THEORY

Near  $T_c$  the transport coefficients  $\eta$  and  $\kappa$  are non-perturbative quantities that have to be extracted from experiment or computed in quantum Monte Carlo calculations. At high temperature (and at very low temperature,

$T \ll T_c$ , see [19]) transport coefficients can be computed in kinetic theory. The shear viscosity was first computed in [20]. Here we will follow the recent work [21] which also considers the frequency dependence of the shear viscosity.

In kinetic theory the stress tensor is given by

$$\Pi_{ij} = 2 \int \frac{d^3 p}{(2\pi)^3} \frac{p^i p^j}{m} f_p, \quad (16)$$

where  $f_p = f(t, x, p)$  is the distribution function of fermion quasi-particles and the factor 2 is the spin degeneracy. The equation of motion for  $f_p$  is the Boltzmann equation. In order to extract the shear viscosity it is useful to consider the Boltzmann equation in a background gravitational field. In this setting correlation functions of the stress tensor can be determined by computing variational derivatives with respect to the background metric. The non-relativistic limit of the Boltzmann equation in a curved space characterized by the metric  $g_{ij}$  is

$$\left( \frac{\partial}{\partial t} + \frac{p^i}{m} \frac{\partial}{\partial x^i} - \left( g^{il} \dot{g}_{lj} p^j + \Gamma_{jk}^i \frac{p^j p^k}{m} \right) \frac{\partial}{\partial p^i} \right) f(t, x, \mathbf{p}) = C[f], \quad (17)$$

where  $\Gamma_{jk}^i$  is the Christoffel symbol and  $C[f]$  is the collision integral. We consider small deviations from equilibrium and write  $f = f_0 + \delta f$  with  $f_0(\mathbf{p}) = f_0(p^i p^j g_{ij} / (2mT))$ . We also write  $g_{ij} = \delta_{ij} + h_{ij}$  and linearize in  $h_{ij}$  and  $\delta f$ . We get

$$\left( \frac{\partial}{\partial t} + \frac{p^i}{m} \frac{\partial}{\partial x^i} \right) \delta f + \frac{f_0(1-f_0)}{2mT} p^i p^j \dot{h}_{ij} = C[\delta f]. \quad (18)$$

This equation can be solved by making an ansatz for  $\delta f$ . We go to Fourier space and write

$$\delta f(\omega, k, p) = \omega f_0(1-f_0) \frac{p^i p^j}{2mT} \frac{\xi_T h_{ij}^T + \xi_L h_{ij}^L}{\omega - v_p \cdot k + i\epsilon} \quad (19)$$

where  $\xi^{T,L} = \xi^{T,L}(\omega, k)$ ,  $h_{ij}^{T,L}$  are the traceless/trace parts of  $h_{ij}$ , and  $v_p^i = p^i/m$  is the quasi-particle velocity. Inserting this ansatz into the Boltzmann equation we can solve for  $\xi^{T,L}$  and then compute  $\delta f$  and  $T_{ij}$ . Matching the result to hydrodynamics determines the shear viscosity. In the limit  $k \rightarrow 0$  this can be done analytically. The zero frequency limit of the shear viscosity is

$$\eta = \frac{15(mT)^{3/2}}{32\sqrt{\pi}} \begin{cases} 1 & a \rightarrow \infty \\ 1/(3mTa^2) & a \rightarrow 0 \end{cases}. \quad (20)$$

We observe that the shear viscosity is large in the weak coupling limit  $a \rightarrow 0$ , and that  $\eta$  decreases as the scattering length is increased. We note, however, that the shear

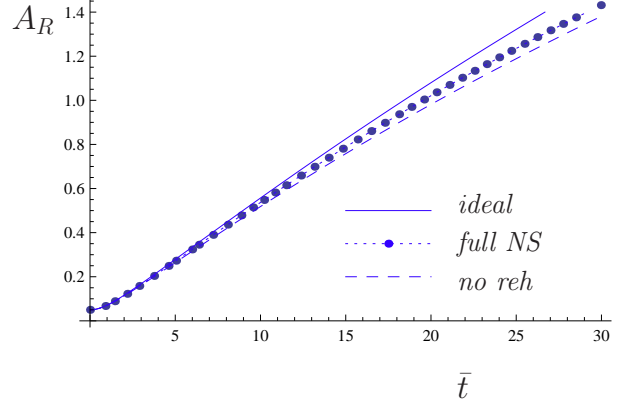


**FIGURE 1.** Time evolution of the aspect ratio  $A_R$  of a deformed cloud as a function of the dimensionless time variable  $\bar{t} = \omega_{\perp} t$ , where  $\omega_{\perp}$  is the harmonic oscillator constant of the transverse confining potential. The solid lines show the analytical result for the ideal evolution, the dashed lines correspond to the dissipative solution without reheating, and the dotted line shows the solution of equ. (26-29). The points are from a numerical solution of the hydrodynamic equations. The viscosity parameter is  $\beta = 0.066$ , see equ. (30).

viscosity saturates when the scattering length becomes comparable to the de Broglie wave length  $a \sim \lambda_{dB} \sim (mT)^{-1/2}$ . In this limit  $\eta$  only depends on  $\lambda_{dB}$  but not on the density or the scattering length. The frequency dependence of the shear viscosity is

$$\eta(\omega) = \frac{\eta}{1 + \omega^2 \tau^2} \quad (21)$$

where  $\tau = (3\eta)/(2\varepsilon)$  is the relaxation time [22]. The relaxation time controls the time scale over which the viscous stress tensor relaxes to the Navier-Stokes form given in equ. (11). We observe that relaxation is fast in the limit where the viscosity is small. We also observe that the viscosity satisfies a sum rule which only depends on thermodynamic quantities,

$$\frac{1}{\pi} \int_0^{\infty} d\omega \eta(\omega) = \frac{\varepsilon}{3}. \quad (22)$$

A modified version of this sum rule which contains an extra short time (high frequency) contribution can be proven in the full quantum theory [23].

## ELLIPTIC FLOW

The first experiment that demonstrated nearly perfect fluidity in the dilute Fermi gas was the observation of elliptic flow by O'Hara et al. [24]. The experiment involves releasing the Fermi gas from a deformed, cylindrically

symmetric, trap. The density evolves as

$$n(x_{\perp}, x_z, t) = \frac{1}{b_{\perp}^2(t)b_z(t)} n_0(x_{\perp}b_{\perp}(t), x_z b_z(t)), \quad (23)$$

where  $x_{\perp}, x_z$  are the transverse and longitudinal coordinate,  $b_{\perp}(t), b_z(t)$  are scale factors, and  $n_0(x_{\perp}, x_z)$  is the equilibrium density of the trapped system. The initial system is strongly deformed,  $A_R(0) = [\langle x_{\perp}^2 \rangle / \langle x_z^2 \rangle]^{1/2} \ll 1$ . Hydrodynamic evolution converts the large transverse pressure gradient into transverse flow. As a consequence the aspect ratio  $A_R(t)$  grows with time and eventually becomes larger than one, see Figs. 1,2.

Viscosity slows down the transverse expansion of the system. In order to quantify the effect of shear viscosity we have to solve the Navier-Stokes equation for the expanding cloud [25, 26]. The Navier-Stokes equation is

$$m \left( \frac{\partial}{\partial t} + \vec{v} \cdot \vec{\nabla} \right) v_i = f_i + \frac{\nabla_j (\eta \sigma_{ij})}{n}, \quad (24)$$

where  $f_i = (\nabla_i P)/m$  is the force. With the help of the Navier-Stokes equation the energy equation can be written as

$$\left( \frac{\partial}{\partial t} + \mathbf{v} \cdot \nabla + \frac{2}{3} (\vec{\nabla} \cdot \vec{v}) \right) f_i + (\nabla_i v_j) f_j - \frac{5}{3} (\nabla_i \nabla_j v_j) \frac{P}{n} = -\frac{2}{3} \frac{\nabla_i \dot{q}}{n}, \quad (25)$$

where  $\dot{q} = \frac{\eta}{2} (\sigma_{ij})^2$  is the heating rate. In general these equations have to be solved numerically on a finite grid. In [26] we showed that under certain assumptions a very accurate scaling solution can be derived. We will assume that the local shear viscosity is proportional to the density,  $\eta = \alpha_n n$ , where  $\alpha_n$  is a constant. We will also assume that the systems remains isothermal and that heat conductivity is not important.

The basic idea is to postulate that the velocity field and the force are linear in the coordinates. If the velocity is linear and  $\eta \sim n$  then all terms in equ. (24) are linear in  $x_i$ . Also, equ. (25) is independent of the pressure and all the remaining terms are linear in  $x_i$ . We write  $f_i = a_i x_i$ ,  $v_i = \alpha_i x_i$  (no sum over  $i$ ) and use the scaling ansatz (23) for the density. The continuity equation requires  $\alpha_i = \dot{b}_i / b_i$ . The scale parameters  $a_i$  and  $b_i$  are determined by the coupled equations

$$\frac{\ddot{b}_{\perp}}{b_{\perp}} = a_{\perp} - \frac{2\beta\omega_{\perp}}{b_{\perp}^2} \left( \frac{\dot{b}_{\perp}}{b_{\perp}} - \frac{\dot{b}_z}{b_z} \right), \quad (26)$$

$$\frac{\ddot{b}_z}{b_z} = a_z + \frac{4\beta\lambda\omega_z}{b_z^2} \left( \frac{\dot{b}_{\perp}}{b_{\perp}} - \frac{\dot{b}_z}{b_z} \right), \quad (27)$$

$$\dot{a}_{\perp} = -\frac{2}{3} a_{\perp} \left( 5 \frac{\dot{b}_{\perp}}{b_{\perp}} + \frac{\dot{b}_z}{b_z} \right)$$

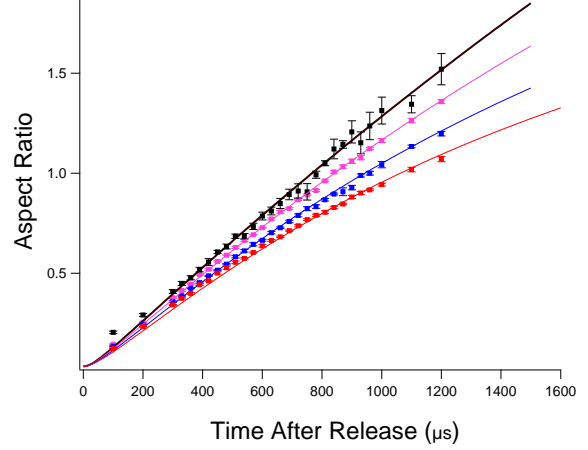


**FIGURE 2.** Data for the aspect ratio versus time, from [27]: Top Black,  $E = 0.6 E_F$ ; Pink,  $E = 2.3 E_F$ ; Blue,  $E = 3.3 E_F$ ; Bottom Red,  $E = 4.6 E_F$ . Solid curves: Hydrodynamic theory with the viscosity as the fit parameter.

$$+ \frac{8\beta\omega_{\perp}^2}{3b_{\perp}} \left( \frac{\dot{b}_{\perp}}{b_{\perp}} - \frac{\dot{b}_z}{b_z} \right)^2, \quad (28)$$

$$\dot{a}_z = -\frac{2}{3} a_z \left( 4 \frac{\dot{b}_z}{b_z} + 2 \frac{\dot{b}_{\perp}}{b_{\perp}} \right) + \frac{8\beta\lambda\omega_z}{3b_z^2} \left( \frac{\dot{b}_{\perp}}{b_{\perp}} - \frac{\dot{b}_z}{b_z} \right)^2, \quad (29)$$

where  $\omega_{\perp}, \omega_z$  are the oscillator frequencies of the harmonic confinement potential (before the gas is released). The parameter  $\beta$  is defined by

$$\beta = \frac{\alpha_n}{(3N\lambda)^{1/3} (E_0/E_F)}, \quad (30)$$

where  $N$  is the number of atoms,  $\lambda = A_R(0)$  the initial aspect ratio, and  $E_0/E_F$  the initial energy in units of  $E_F = (3N\lambda)^{1/3} N \omega_{\perp}$ . The initial conditions are  $b_{\perp}(0) = b_z(0) = 1$ ,  $\dot{b}_{\perp}(0) = \dot{b}_z(0) = 0$ , and  $a_{\perp}(0) = \omega_{\perp}^2$ ,  $a_z(0) = \omega_z^2$ .

Dissipative effects fall into two categories. The terms proportional to  $\beta$  in equ. (26,27) correspond to friction – shear viscosity slows down the expansion in the transverse direction. The dissipative terms in equ. (28,29) describe reheating – shear viscosity converts some kinetic energy to heat which increases the pressure and eventually re-accelerates the system. The interplay between these two effects can be seen in Fig. 1. As expected, friction slows down the growth of  $A_R(t)$  as compared to the ideal evolution. Reheating reduces this effect by about a factor of 2. We also note that the solution of the equ.(26-29) agrees very well with numerical solutions on a three dimensional grid.

In order to make comparisons with data we have to take into account that  $\alpha_n$  is not a constant. In [25, 26]

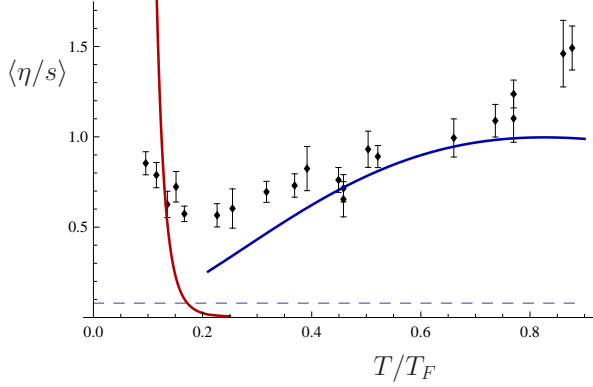


**FIGURE 3.** Trap average  $\langle \alpha_s \rangle = \langle \eta/s \rangle$  extracted from the damping of the radial breathing mode. The data points were obtained using equ. (33) to analyze the data published by Kinast et al. [28]. The thermodynamic quantities  $(S/N)$  and  $E_0/E_F$  were taken from [11]. The solid red and blue lines show the expected low and high temperature limits. Both theory curves include relaxation time effects.

we argued that  $\alpha_n$  in equ. (30) should be interpreted as the trap average of the local ratio of shear viscosity over density,

$$\langle \alpha_n \rangle = \frac{1}{N} \int d^3x \alpha_n \left( \frac{mT}{n_0(x)^{2/3}} \right) n_0(x). \quad (31)$$

In the dilute corona of the cloud the local shear viscosity is independent of the density and equ. (31) is not well defined. This problem can be addressed by taking into account that the viscous stresses relax to the Navier-Stokes value on a time scale  $\tau$  that becomes large as the density goes to zero, see equ. (21). A relaxation model for  $\langle \alpha_n \rangle$  was studied in [25]. An even simpler model can be constructed based on the assumption that the shear viscosity relaxes to its equilibrium value at the center of the trap and is proportional to the density in the dilute corona. This implies that  $\eta(x) = \eta(0)(n(x)/n(0))$ . This parametrization agrees with the relaxation model at the 30% level. It was used by Cao et al. [27] to analyze the data shown in Fig. 2. The hydrodynamic curves shown in Fig. 2 were obtained with  $\eta = \eta_0(mT)^{3/2}$  and  $\eta_0 = 0.33$ . This agrees quite well with the prediction of kinetic theory  $\eta_0 = 15/(32\sqrt{\pi}) \simeq 0.26$ , see equ. (20).

## COLLECTIVE MODES

At temperatures  $T < T_F$  dissipative effects on elliptic flow are very small. In this regime accurate measurements of the shear viscosity can be obtained by analyzing the damping of collective modes [28, 29, 30]. The analysis presented in the previous section can easily be extended to that case. A solution that describes a radial

breathing mode is given by

$$b_{\perp}(t) = 1 + a_{\perp} \cos(\omega t) \exp(-\beta \omega_{\perp} t). \quad (32)$$

where  $a_{\perp} \ll 1$  is the amplitude,  $\omega = (10/3)^{1/2} \omega_{\perp}$  is the frequency, and  $\beta$  is the parameter defined in equ. (30). The experimentally measured damping rate  $\Gamma$  can be used to estimate  $\langle \alpha_n \rangle$ . We find [25]

$$\langle \alpha_n \rangle = (3\lambda N)^{1/3} \left( \frac{\Gamma}{\omega_{\perp}} \right) \left( \frac{E_0}{E_F} \right). \quad (33)$$

In order to compare with the heavy ion data and the proposed string theory bound it is interesting to convert the ratio  $\eta/n$  to the ratio  $\eta/s$  of shear viscosity to entropy density. This can be done using measurements of entropy per particle published in [11]. In Fig. 3 we show an analysis of the collective mode data obtained by Kinast et al. [28] using equ. (33). The solid lines show the prediction of kinetic theory in the limits  $T \ll T_F$  and  $T \gg T_F$ . We observe that  $\eta/s$  is consistent with kinetic theory for  $T \gtrsim 0.5T_F$ . We also find that in this regime the data from collective modes are in agreement with the results based on the elliptic flow data [27]. The data do not show the expected behavior at very low temperature. We should note, however, that for  $T \ll T_F$  the mean free path is very large and dissipative hydrodynamics is not applicable.

We observe that  $\eta/s$  reaches a minimum close to the phase transition temperature, and that the minimum value is  $\eta/s \simeq 0.5$  (in units of  $\hbar = k_B = 1$ ). We emphasize that this result refers to trap averaged quantities. We expect that improved data will allow us to determine the local value of the ratio  $\eta/s$ .

## CONCLUSIONS AND OUTLOOK

There are a number of issues that need to be addressed before an accurate value of  $\eta/s$  with fully controlled errors can be obtained. The most important of these is a better description of the transition from nearly perfect fluid dynamics in the center of the cloud to kinetic behavior in the dilute corona.

On the theoretical side we need to develop tools that will allow us to perform calculations of transport properties in the strongly coupled regime. Some steps in this direction have been taken. Taylor and Randeria derived sum rules for the viscosity spectral function [23]. Enns, Haussmann and Zwerger developed a resummed diagrammatic scheme that respects the sum rule and reproduces the kinetic limit [31]. There have also been some attempts at extending the AdS/CFT correspondence to non-relativistic conformally invariant theories, see [32, 33].

Finally, we would like to understand how nearly perfect fluidity arises in different physical systems. In the case of the quark gluon plasma the question is whether nearly perfect fluidity is caused by strong interactions between well-defined quark and gluon quasi-particles, or whether the quasi-particle picture breaks down completely and the low energy description involves non-local degrees of freedom, as in the AdS/CFT correspondence. In the case of the dilute Fermi gas we would like to understand whether momentum transport is governed by fermionic quasi-particles, by collective modes (like the roton in liquid Helium), or whether there is no quasi-particle description at all. This question is difficult to address experimentally, but it can be studied numerically, by computing the viscosity spectral function. These calculations are still in their infancy, but we expect significant progress in the near future.

## ACKNOWLEDGMENTS

This work was supported in parts by the US Department of Energy grant DE-FG02-03ER41260. Part of the work reported here was done in collaboration with M. Braby, C. Chafin, J. Chao and J. Thomas.

## REFERENCES

1. S. S. Adler *et al.* [PHENIX Collaboration], Phys. Rev. Lett. **91**, 182301 (2003) [arXiv:nucl-ex/0305013].
2. B. B. Back *et al.* [PHOBOS Collaboration], Phys. Rev. C **72**, 051901 (2005) [arXiv:nucl-ex/0407012].
3. J. Adams *et al.* [STAR Collaboration], Phys. Rev. C **72**, 014904 (2005) [arXiv:nucl-ex/0409033].
4. K. Dusling and D. Teaney, Phys. Rev. C **77**, 034905 (2008) [arXiv:0710.5932 [nucl-th]].
5. P. Romatschke and U. Romatschke, Phys. Rev. Lett. **99**, 172301 (2007) [arXiv:0706.1522 [nucl-th]].
6. G. Policastro, D. T. Son and A. O. Starinets, Phys. Rev. Lett. **87**, 081601 (2001) [arXiv:hep-th/0104066].
7. P. Kovtun, D. T. Son and A. O. Starinets, Phys. Rev. Lett. **94**, 111601 (2005) [arXiv:hep-th/0405231].
8. I. Bloch, J. Dalibard, W. Zwerger, Rev. Mod. Phys. **80**, 885 (2008) [arXiv:0704.2511].
9. S. Giorgini, L. P. Pitaevskii, S. Stringari, Rev. Mod. Phys. **80** 1215 (2008) [arXiv:0706.3360].
10. T. Schäfer and D. Teaney, Rept. Prog. Phys. **72**, 126001 (2009) [arXiv:0904.3107 [hep-ph]].
11. L. Luo, J. E. Thomas, J. Low Temp. Phys. **154**, 1 (2009), [arXiv:0811.1159[cond-mat.other]].
12. S. Nascimbene, N. Navon, K. Jiang, F. Chevy, C Salomon, Nature **463**, 1057 (2010) [arXiv:0911.0747[cond-mat.quant-gas]].
13. M. Horikoshi, S. Nakajima, M. Ueda, T. Mukaiyama1, Science Vol. 327, No. **5964**, 442 (2010).
14. D. Lee and T. Schäfer, Phys. Rev. C **73**, 015202 (2006) [arXiv:nucl-th/0509018].
15. E. Burovski, N. Prokof'ev, B. Svistunov, M. Troyer, Phys. Rev. Lett. **96**, 160402 (2006) [cond-mat/0602224].
16. A. Bulgac, J. E. Drut and P. Magierski, Phys. Rev. A **78**, 023625 (2008) [arXiv:0803.3238 [cond-mat.stat-mech]].
17. D. T. Son, Phys. Rev. Lett. **98**, 020604 (2007) [arXiv:cond-mat/0511721].
18. M. Braby, J. Chao and T. Schäfer, Phys. Rev. **A82**, 033619 (2010). [arXiv:1003.2601 [cond-mat.quant-gas]].
19. G. Rupak and T. Schäfer, Phys. Rev. A **76**, 053607 (2007) [arXiv:0707.1520 [cond-mat.other]].
20. G. M. Bruun, H. Smith, Phys. Rev. A **72**, 043605 (2005) [cond-mat/0504734].
21. M. Braby, J. Chao and T. Schäfer, preprint [arXiv:1012.0219 [cond-mat.quant-gas]].
22. G. M. Bruun, H. Smith Phys. Rev. A **76**, 045602 (2007) [arXiv:0709.1617].
23. E. Taylor and M. Randeria, Phys. Rev. A **81**, 053610 (2010) [arXiv:1002.0869 [cond-mat.quant-gas]].
24. K. M. O'Hara, S. L. Hemmer, M. E. Gehm, S. R. Granade, J. E. Thomas, Science **298**, 2179 (2002) [cond-mat/0212463].
25. T. Schäfer and C. Chafin, Lecture Notes in Physics, in press (2010) arXiv:0912.4236 [cond-mat.quant-gas].
26. T. Schäfer, Phys. Rev. A, in press (2010) [arXiv:1008.3876 [cond-mat.quant-gas]].
27. C. Cao, E. Elliott, J. Joseph, H. Wu, J. Petricka, T. Schäfer, J. E. Thomas, Science DOI: 10.1126/science.1195219, arXiv:1007.2625 [cond-mat.quant-gas].
28. J. Kinast, A. Turlapov, J. E. Thomas, Phys. Rev. A **70**, 051401(R) (2004) [cond-mat/0408634].
29. T. Schäfer, Phys. Rev. A **76**, 063618 (2007) [arXiv:cond-mat/0701251].
30. A. Turlapov, J. Kinast, B. Clancy, L. Luo, J. Joseph, J. E. Thomas, J. Low Temp. Phys. **150**, 567 (2008) [arXiv:0707.2574].
31. T. Enss, R. Haussmann and W. Zwerger, preprint [arXiv:1008.0007 [cond-mat.quant-gas]].
32. K. Balasubramanian and J. McGreevy, Phys. Rev. Lett. **101**, 061601 (2008) [arXiv:0804.4053 [hep-th]].
33. D. T. Son, Phys. Rev. D **78**, 046003 (2008) [arXiv:0804.3972 [hep-th]].